Article

Study and Characterization of H₃PO₄ Activated Carbons Prepared from Jujube Stones for the Treatment of Industrial Textile Effluents

Nasma Bouchelkia [1,2], Kheira Benazouz [1,2], Amal Mameri [2], Lazhar Belkhiri [3], Nadia Hamri [2,4], Hayet Belkacemi [5], Abdelhalim Zoukel [6,7], Abdeltif Amrane [8], Fodil Aoulmi [9] and Lotfi Mouni [2,*]

1   Département de Génie des Procédés, Faculté de Technologie, Université de Bejaia, Bejaia 06000, Algeria;
    nasma.bouchelkia@univ-bejaia.dz (N.B.)
2   Laboratory of Management and Valorization of Natural Resources and Quality Assurance, SNVST Faculty,
    Akli Mohand Oulhadj University, Bouira 10000, Algeria; nadia.hamri@univ-bejaia.dz (N.H.)
3   Laboratory of Applied Research in Hydraulics, University of Mustapha Ben Boulaid of Batna 2,
    Batna 05000, Algeria; belkhiri.la@gmail.com
4   Département de Chimie, Faculté des Sciences Exactes, Université de Bejaia, Bejaia 06000, Algeria
5   Technology Laboratory of Materials and Process Engineering (LTMGP), University of Bejaia,
    Bejaia 06000, Algeria; hayet.belkacemi@univ-bejaia.dz
6   Laboratory Physico-Chemistry of Materials, Laghouat University, Laghouat 03000, Algeria;
    ab.zoukel@lagh-univ.dz
7   Center for Scientific and Technical Research in Physicochemical Analysis (PTAPC, Laghouat-CRAPC),
    Laghouat 03000, Algeria
8   Univ Rennes, Ecole Nationale Supérieure de Chimie de Rennes, CNRS, ISCR–UMR6226,
    F-35000 Rennes, France; abdeltif.amrane@univ-rennes1.fr
9   Center for Scientific and Technical Research in Physicochemical Analysis, CRAPC, BP 384,
    Bou-Ismail, Tipaza 42004, Algeria
*   Correspondence: l.mouni@univ-bouira.dz

Abstract: Dyes are responsible for major environmental issues globally due to their toxicity, large-scale production, and extensive use in various industrial sectors. Pollution caused by hazardous dyes is mainly due to textile waste, which is constantly discharged into the aquatic system, often causing harm to humans and affecting water quality. In recent years, the removal of dyes from industrial textile wastewater has been a major challenge. Numerous technologies and methods have been developed to remove dyes from wastewater and meet clean water requirements. In this study, the effectiveness of activated carbon prepared by chemical activation of jujube stones for textile wastewater treatment was investigated. The effects of the concentration of H₃PO₄ and the carbonization temperature on the activated carbon's properties were studied. Several physicochemical methods, including Fourier-transform infrared spectroscopy (FTIR), scanning electron microscopy (SEM), X-ray diffraction, methylene blue index, Boehm titration, iodine index and pH point of zero charge, were considered to characterize the produced adsorbents. To assess the quality of the two studied textile effluents (Mustard and Violet), the following parameters were used: biological oxygen demand (BOD), chemical oxygen demand (COD), turbidity, suspended particles and dissolved solids, before and after treatment with the produced activated carbon. Untreated wastewater analysis revealed high values for almost all parameters: pH > 9, COD of 302.72 mg/L and 230.68 mg/L for Mustard and Violet effluent, respectively. Both effluents from an industrial textile factory exhibited a COD/BOD ratio higher than three, which restricts their biodegradability. Examination of the effect of contact time and activated carbon dosage on the treatment of the two effluents showed that 4 g/L of activated carbon and 60 min of contact time were sufficient for optimal treatment, resulting in pollutant removal rates of 81.03 and 84.65% for the Violet and Mustard effluents, respectively. The results of this research highlight the efficiency of activated carbon derived from jujube stones as a cost-effective adsorbent for the treatment of real textile wastewater.

Keywords: activated carbon; adsorption; chemical activation; wastewater treatment; textile effluent

1. Introduction

The need for dyes in the textile industry has expanded due to the growing demand for colorful fabrics. Nowadays, synthetic dyes have replaced natural dyes, which are no longer sufficient to meet the growing demand. However, the problem with synthetic dyes is their toxicity and harmfulness to the environment [1]. The textile industry releases around 54% of harmful dyes into water bodies [2,3]. The industry consumes a lot of water, especially during the dyeing and finishing processes, generating large quantities of wastewater laden with toxic and dangerous chemicals that cause unequivocal ecological deterioration and represent an increasingly worrying threat [4]. In fact, aqueous dyeing generates effluent that contains dyes, dispersants, wetting agents, salts and other textile auxiliary materials [5]. The discharge of such effluents in the receiving medium causes damage to the ecosystem and human health [6]; their color and their high turbidity affect the appearance of the effluent and are therefore contested by the public as a sign of pollution [7]. They also limit the penetration into the water of crucial elements for the existence of all living organisms, namely sunlight, and therefore reduce oxygen production by photosynthesis of marine and underwater plants and negatively affect aquatic life [6,8]. In addition, dyes have recalcitrant molecular structures, which make them inert and difficult to degrade when released into the waste stream [9]. The complex chemical structure of dyes and the presence of toxic heavy metals, dissolved solids, detergents, fixing agents, emulsifiers and softeners in the effluent increase the chemical oxygen demand (COD), pH and biological oxygen demand (BOD); this generates chemical and biological modifications of the ecosystem [6–8]. Moreover, these products are toxic and cancerogenic; they can cause eye burns, skin irritations and allergic conjunctivitis [3]. Al-Tohamy et al. [10] have well detailed the harmful effects of textile wastewater on human health and the environment. In short, the uncontrolled discharge of textile effluents affects both marine animals, algae and microorganisms, as well as humans and animals, soil and plants. The release of organic and mineral elements and the disruption of the photosynthesis of marine plants causes the phenomenon of eutrophication and provokes excessive proliferation of marine plants and increases the consumption of organic matter by bacteria. The increased concentrations of suspended solids prevent fish from exchanging gases by impeding the passage of water via their gills, which results in a slowdown in their growth or in their death. Irrigation of agricultural land by wastewater negatively impacts germination and plant development; pollutants infiltrate into the soil and can be absorbed by plants, affecting chlorophyll levels and slowing down plant growth and development. Human and animal health are also highly affected by textile effluents; dyes and many other harmful substances can be detected throughout the food chain due to their excessive and uncontrolled use. The consumption of affected marine fruits and plants can be harmful to human and animal health. They can induce significant genotoxic effects in the long term and impair immunity. Long-term exposure to dyes has serious negative impacts on human beings by inducing significant genotoxic, cytotoxic and immunological effects, including the development of certain cancers like bladder, colon and colorectal cancers, as well as DNA damage, apoptosis, mitotic poisoning, chemical cystitis, irritated skin, digestive tracts and respiratory and renal failure [10]. All these negative effects explain the multiple efforts and the strict limits and standard levels that have been imposed by many countries to control and monitor the quality of wastewater discharged into drains and watercourses [11]. Several programs have been proposed in different countries to control textile effluents and constantly monitor their quality as well as to comply with regulations and standards to ensure the protection of water resources against any dangerous pollution liable to harm the ecosystem [1]. Many researchers around the world are constantly working to stop this danger that threatens our environment and health by developing a variety of methods for removing the textile dyes [12], including the following: (1) physical methods such as ion exchange [13], adsorption [14] and membrane filtration [15,16]; (2) chemical methods as coagulation–flocculation [17] and advanced oxidation processes (AOPs) [18]; (3) electrochemical methods such as electro Fenton [19] and electrocoagulation [20] and (4) biological methods such as enzyme-assisted

degradation [21], bacteria-assisted degradation [22] and many other methods. Among all these methods, adsorption is one of the efficient techniques widely used as a physical approach. Its principle is based on the transfer of pollutants from one phase (liquid or gas) to another (solid) [3]. Due to its simplicity and excellent performance, adsorption is considered to be one of the most promising technologies for dye removal [23]. It is used to effectively remove a wide range of toxic compounds and to treat industrial wastewater, all while respecting the environmental and economic aspects [3,14]. Zeolites [24], alumina [25], silica gel [26], cellulose-based waste [27] and activated carbon [28,29] are frequently utilized for eliminating dyes from water. Several parameters, including the nature of the adsorbent and the adsorbate might influence the adsorption process [30]. Adsorbents are subdivided into natural adsorbents (such as cellulosic materials), synthetic adsorbents like zeolite and semi-synthetic adsorbents produced by chemical and physical modification of natural materials to improve their adsorption characteristics [31,32]. Many parameters influence adsorbents' reliability, the most important of which are their cost, availability, ease of operation, lack of toxicity, specific surface area and pore structure, as well as the availability of surface functional groups [30]. The adsorbent's size also has an impact on the adsorption process [31]. Daniel et al. [33] have shown the influence of the particle size of activated carbon prepared by acid activation on the adsorption of methylene blue. When it comes to the adsorbate's properties, the characteristics with the greatest impact on the adsorption process include molecular size, solubility, pKa and the type of substituent (like in the case of aromatic compounds) [34]. In general, industrial wastewater may contain several adsorbates, which complicates the analysis and understanding of the adsorption process. Several investigations have been carried out to better understand multi-component adsorbate systems. For example, Regti et al. [35] studied the individual and simultaneous removal of two textile dyes, BB41 and BY28, from aqueous solutions and showed different behavior of the two adsorbates in single compounds and binary systems. Similarly, Erto et al. [36] studied the simultaneous adsorption of toluene and benzene in commercial activated carbon and demonstrated preferential adsorption of toluene over benzene in both individual and binary systems.

Due to the properties of activated carbon that support effective and quick treatment, it has always garnered attention and is frequently used for the elimination of various environmentally detrimental industrial contaminants. A good activated carbon is mostly characterized by a large specific surface and a high pore volume with a well-developed porous structure offering various functional surface sites [14,37]. In order to lower the high cost of commercial activated carbons, adsorbents derived from biowaste materials have been successfully developed; numerous research studies have been reported in the literature that use various wastes including fruit peel (cactus fruit peel) [38], fava bean peel [39], orange and lemon peel [40], Moringa oleifera [41], coffee husk [42], spent coffee grounds [43], wood [44,45], wheat straw [46] and fruit stones [28,47,48]. Various investigations have examined the impact of preparation parameters on the properties of activated carbon obtained from biowaste materials; Wickramaarachchi et al. [49] have prepared activated carbons by carbonizing mango seed waste under inert flux at a temperature of 600 °C, followed by chemical activation with KOH of the obtained biochar at various temperatures ranging from 800 to 1100 °C. The activation temperature of the mango seed husks improved activated carbon characteristics, such as surface area, pore volume and the graphitic orientation of the activated carbon. Wickramaarachchi et al. [50] have also prepared four activated carbons by chemical activation of grape marc (GM) using KOH and $ZnCl_2$ as activating agents. The results showed the performances of the activated carbon prepared with KOH compared with $ZnCl_2$. On the other hand, the activated carbon produced by mixing GM with urea (for nitrogen doping) and then activated with KOH further improved the physicochemical properties.

This study focused on using an inexpensive, abundant and unexploited agricultural waste, jujube stone, to prepare activated carbon for use as an adsorbent to treat textile wastewater. As shown in Figure 1, the preparation of the activated carbon involved a few

main steps: (1) pretreatment including washing, drying, grinding and sieving; (2) chemical activation with phosphoric acid at different concentrations (30 to 85%) and finally (3) carbonization in a muffle furnace at temperatures ranging from 500 to 700 °C. The resulting activated carbons were then washed, dried, ground and sieved. After characterization, activated carbon was used to treat wastewater from a textile factory situated in the northeast of Algeria. Figure 1 shows the color of the two effluents before treatment.
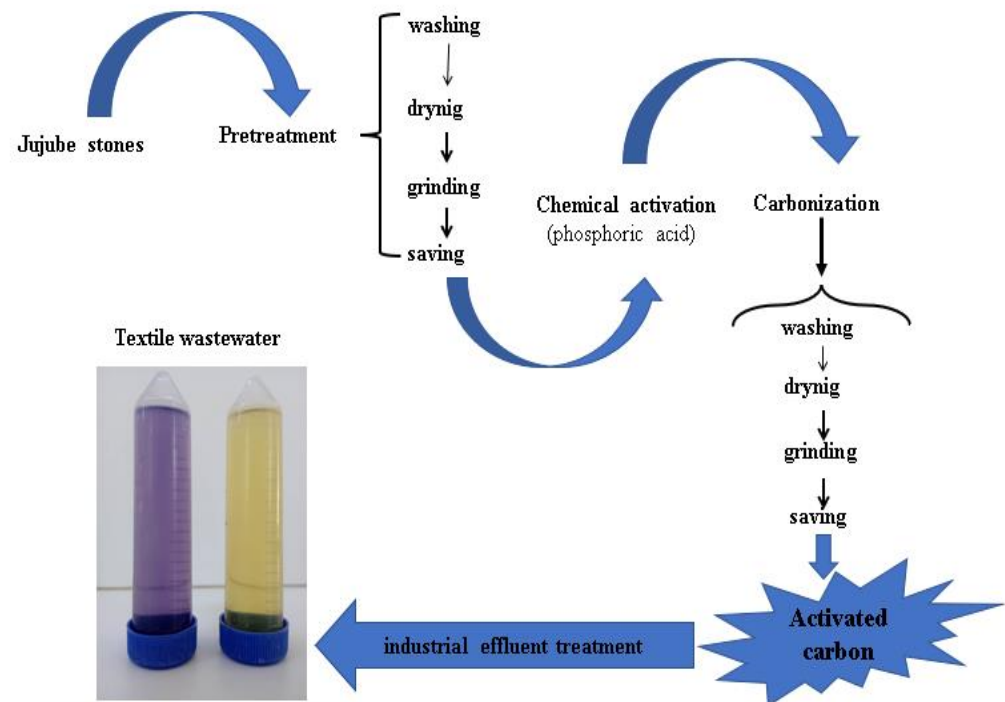

Figure 1. Steps of activated carbons preparation.

To the best of our knowledge, this work is structurally unique and is one of the few devoted to the study of the adsorption of real textile effluents. In general, the majority of dye adsorption research papers are structured in the classical way in which a synthetic solution is prepared either by a laboratory-grade commercial dye or by a powder dye recovered from the textile industry. Adsorption on simulated industrial waters has also been widely reported in the literature [51].

2. Materials and Methods

All reagents were of analytical quality and did not require further purification before use.

2.1. Wastewater Samples

The effluents treated in this study were obtained from a local textile factory located approximately 70 km from the chief town of Bejaia in the northeast of Algeria. The textile production process followed at this factory consists of three main stages: spinning, weaving and finishing. The spinning stage allows the transformation of raw materials into threads of different diameters. Weaving allows the formation of the fabric (the unbleached fabric) by the assembly of the threads, while finishing encompasses washing, dyeing of the unbleached fabric and producing the final product. The effluents analyzed in this study were recovered from the finishing department. The characteristics of factory effluents may vary depending on the dyes used in the manufacturing process. In this study, the samples were collected throughout the month of February 2023 where the generated wastewaters were colored with mustard (hereafter named Mustard effluent) and violet (hereafter named Violet effluent). The collected wastewater were homogenized and analyzed in order to determine the values of pH, temperature and dissolved solids

(using a Hanna HI9829 multimeter, Hanna Instruments, Smithfield, RI, USA), as well as turbidity (using a Hanna HI93703 turbidimeter, Hanna Instruments), BOD_5 (at 20 °C after 5 dyes using a WTW OxiTop-12 Respirometric BOD Measuring System, Xylem, Weilheim, Germany), COD (according to ISO 6060:1989) and suspended solids (using a WTW PhotoLab 6100 Visible Spectrophotometer, Xylem, Weilheim, Germany). The samples were then kept in a refrigerator at 4 °C for further use.

2.2. Preparation and Characterization of Activated Carbons

The jujube stones used in this study were obtained from jujube collected from the region of Bouira, Algeria. The separated stones were washed, dried, crushed, sieved and chemically activated with phosphoric acid (H_3PO_4) at purities ranging from 30 to 85%, with an impregnation rate of 1/1 by weight. They were then carbonized in a WiseTherm furnace for one hour. The carbonization temperatures varied between 500 and 700 °C. The obtained activated carbons (hereafter named ACs) were then neutralized with distilled water, dried and sieved to obtain particles with diameters less than 100 μm and were stored in a desiccator. The prepared ACs were coded as ACab/c where "ab" represents the H_3PO_4 concentration and may be 30, 50 or 85%. "c" indicates the carbonization temperature and can be 5 (for 500 °C), 6 (for 600 °C) or 7 (for 700 °C).

To characterize the prepared ACs, the ash, moisture, volatile matter and fixed carbon contents were determined according to ASTM D2866-70, ASTM D2867-70, ISO 562-1981 and ASTM D3172, respectively. The pHpzc, methylene blue index and specific surface area (S_{MB}) were also determined as described in our previous work [14]. The standard method AATM 1112-01 was used to determine the iodine number. It is given as described by Ahmed and Dhedan [52]. The basic and oxygenated acidic functional groups present in the surface of the prepared ACs can be quantified using the Boehm titration given as follows: 0.15 g of the dry activated carbon was added to 50 mL of each of the aqueous solutions of NaOH, Na_2CO_3, $NaHCO_3$ and HCl of 0.01 N concentration. To ensure maximum reaction of the biomass surface groups, each solution was agitated for 24 h. The basic solutions were then determined by 0.01 N hydrochloric acid, while the acidic solution was determined by 0.01 N sodium hydroxide after filtration [28,53].

FTIR analysis was performed on a PerkinElmer Spectrum. A range of 4000 cm^{-1} to 400 cm^{-1} was recorded for the spectra, and the adsorbent powders did not need to be pretreated prior to analysis.

The X-ray diffraction (XRD) analysis was performed on a Malvern Panalytical X'pert Pro (Malvern Panalytical, Malvern, UK) analyzer to characterize the prepared ACs crystallographically. Patterns were recorded in 2θ angles ranging from 10° to 80° with a scanning rate of 0.02° step.

The ACs surface morphology was analyzed by using SEM (scanning electron microscopy) on a Thermoscientific Quattro S microscope (Thermo Fisher Scientific, Waltham, MA, USA).

3. Results and Discussion

In this study, a vegetable waste was chosen, jujube stones (hereafter named JS), to produce low-cost activated carbon useful in wastewater treatment processes, particularly for the treatment of effluents coming from the textile industry. The main characteristics of the JS used are listed in Table 1. The results showed that the JS contains a high amount of fixed carbon and volatiles matter, and also a low quantity of ash content, which confirmed that it can be used as promising precursor for adsorbents production [54,55].

Table 1. Characteristics of the jujube stones.

Particle Size (μm)	pHpzc	Moisture Content (%)	Ash Content (%)	Volatile Matter (%)	Fixed Carbon (%)
<100	6.60	7.66	0.86	75.25	16.23

3.1. Effect of H_3PO_4 Concentration on the ACs Characteristics

To study the effect of phosphoric acid concentration on the development of activated carbon surfaces, three activated carbons were prepared by chemical activation at different purities of H_3PO_4: 30, 50 and 85 wt.%. These were then carbonized at a temperature of 500 °C for 1 h. The three produced activated carbons were named AC30/5, AC50/5 and AC85/5, respectively. The characteristics of the three ACs are given in Table 2. The pHpzc indicates the pH value at which the adsorbent surface has zero net charge [14]; from Table 2, it can be observed that an increase in the H_3PO_4 concentration led to a decrease in the pHpzc values. The results in Table 2 also indicate a decrease in the amount of volatile matter and an increase in the fixed carbon content compared to the JS for increasing amounts of H_3PO_4. This can be attributed to the carbonization and activation steps leading to the liberation of the volatile matters and the non-carbon materials as liquids and gas, resulting in the enrichment of the carbon [56,57]. Furthermore, it can be inferred from Table 2 that an increase in the acid concentration led to a decrease in the ash content. The AC85/5 was characterized by the lowest ash content. According to Angin [58], ash content is a measurement of the non-volatile matter and non-combustible components present in the activated carbon. It indicates the quality of the activated carbon in terms of mechanical strength. The presence of a large amount of ash in the activated carbon indicates reduced strength. Additionally, carbon yield percent is affected by ash content; the carbon yield decreases as the ash content of the activated carbon increases [59].

Table 2. Characteristics of the prepared AC.

	AC30/5	AC50/5	AC85/5	AC85/6	AC85/7
pHpzc	6.34	6.10	4.86	5.00	5.90
Moisture content (%)	6.3	6.5	6.9	6.5	5.5
Ash content (%)	3.42	2.97	0.99	1.03	3.81
Volatile matter (%)	71.65	69.37	49.52	45.06	16.04
Fixed carbon (%)	18.63	21.16	42.59	47.41	74.65
Iodine number (mg/g)	663.08	709.21	860.95	867.54	833.48
Methylene blue index (mg/g)	166.86	315.04	338.40	387.61	324.56
S_{MB} (m^2/g)	408.46	771.19	828.37	948.84	794.50
Carboxylic groups (mmol/g)	0.43	0.55	0.62	0.6	0.57
Lactonic groups (mmol/g)	0.16	0.27	0.2	0.25	0.24
Phenolic groups (mmol/g)	0.31	0.38	0.43	0.51	0.41
Total acid (mmol/g)	0.9	1.2	1.25	1.36	1.22
Total basic (mmol/g)	0.11	0.14	0.12	0.15	0.15

The methylene blue index and the specific surface area, as well as the iodine index values increased with the increase in the H_3PO_4 concentration. The best results were obtained for the 85% H_3PO_4 concentration, with an MB index of 338.40 mg/g and an S_{MB} of 828.37 mg/g as well as an iodine number value of 860.95 mg/g, indicating a substantial development of the porosity AC85/5. Yakout et al. [60] have also found that increasing the concentration of the phosphoric acid from 60 to 80% improved the performance of the obtained activated carbons with an enhancement in the BET specific surface area from 257 m^2/g to 1218 m^2/g. The increase in acid concentration may intensify its aggressive physicochemical effects on the JS' lignocellulosic material and may create much porosity [61].

The results of Boehm titration of the three activated carbons AC30/5, AC50/5 and AC85/5 are expressed in mmol/g of material and are presented in Table 2.

The Boehm titration analysis revealed the predominance of acid groups in all three ACs; the activation with 85% H_3PO_4 resulted in higher acidic groups (1.25 mmol/g), whereas 30 and 50% H_3PO_4 contained 0.9 mmol/g and 1.2 mmol/g, respectively.

These results show that pure phosphoric acid (85% by weight) allowed a better activation of the JS, which was considered for the next step, investigating the effect of carbonization temperature.

3.2. Effect of the Temperature of Carbonization on the Characteristics of ACs

Having studied the impact of acid concentration on activated carbon properties and aiming to choose the most efficient activated carbon for textile effluent decolorization, three additional carbons were prepared by chemical activation with pure phosphoric acid (85%) and were subsequently carbonized at different carbonization temperatures: 500 °C (AC85/5), 600 °C (AC85/6) and 700 °C (AC85/7). Table 2 summarizes the characteristics of the three ACs. The results show the increase in the pHpzc with rising the carbonization temperature, although this did not significantly affect the pHpzc values). The same observation was reported by Zhang et al. [54] when increasing the carbonization temperature from 300 to 700 °C. It can also be noticed in Table 2 that ash content and fixed carbon increased with the rise of carbonization temperature, whereas the volatile matter content decreased. These findings are similar to those previously reported [58,62]. The highest methylene blue, S_{MB} and iodine values were obtained at a carbonization temperature of 600 °C, with values of 387.61 mg/g, 948.84 m^2/g and 864.54 mg/g, respectively. Similarly, Table 2 shows also that the carbonization at 600 °C produced an activated carbon with the highest acidic functions quantity. Temperatures above 600 °C are likely to induce an apparent reduction in porosity due to the deterioration of the microporous structure with the increase in temperature resulting in a larger porosity evolution characterized by a smaller internal surface [61].

3.3. FTIR Analysis

The FTIR spectra of the prepared activated carbons are shown in Figure 2. The effect of the activation and carbonization was apparent for all the prepared ACs. In fact, some peaks disappeared, and the intensities of some other peaks decreased compared to the row material JS. The graphs of the activated carbons showed similar spectra with little change in intensity, indicating the same chemical nature of the functional groups [63]. Activation with phosphoric acid and carbonization induced a significant reduction in the intensity of the peak present in the range 3200–3450 cm^{-1} corresponding to the stretching vibrations of the hydroxyl groups (–OH) [64]. The intensity of this peak decreased with increasing phosphoric acid concentration as a result of the increasing elimination of some hydrogen present in the JS [65]. The spectra also showed the disappearance of the C=O group which absorbs at 1744 cm^{-1} and corresponds to the stretching in esters, aldehydes, ketone groups and acetyl derivatives [60,66]. The majority of the peaks present in the interval 1460–1760 cm^{-1} disappeared, such as the peaks 1544 and 1459 cm^{-1} corresponding to the C–H bending and C=C cycle stretching mode of aromatic rings, as well as the peak which absorbs at 1653 cm^{-1} corresponding to the vibration of C=C in aromatic rings. The bands observed in the ACs at around 1580–1600 cm^{-1} can be attributed to the aromatic ring stretching vibrations C=C [67] and to the C=O stretching vibration of carbonyl and lactone groups [68]. The small shift of this band can be related to the broadening of the aromatic ring system when rising the carbonization temperature from 500 to 700 °C [67]. Some peaks present in the region 1000–1300 cm^{-1} corresponding to the C–O and/or C–O–C stretching vibrations in phenols, acids, alcohols, ester and/or ethers groups also disappeared, especially the peaks at 1253 and 1168 cm^{-1} [14]. The graphs also showed a loss of aliphaticity, as confirmed by the reduction and the almost disappearance of the C–H stretching bands observed in the JS at around 2900 and 2800 cm^{-1} [69]. Increasing the phosphoric acid concentration from 30% to 85% induced a decrease in the intensity of these two peaks since H_3PO_4 broke many bonds in the aliphatic and aromatic species present in the precursor material, resulting in the liberation and removal of several light and volatile substrates, leading to partial aromatization [66].
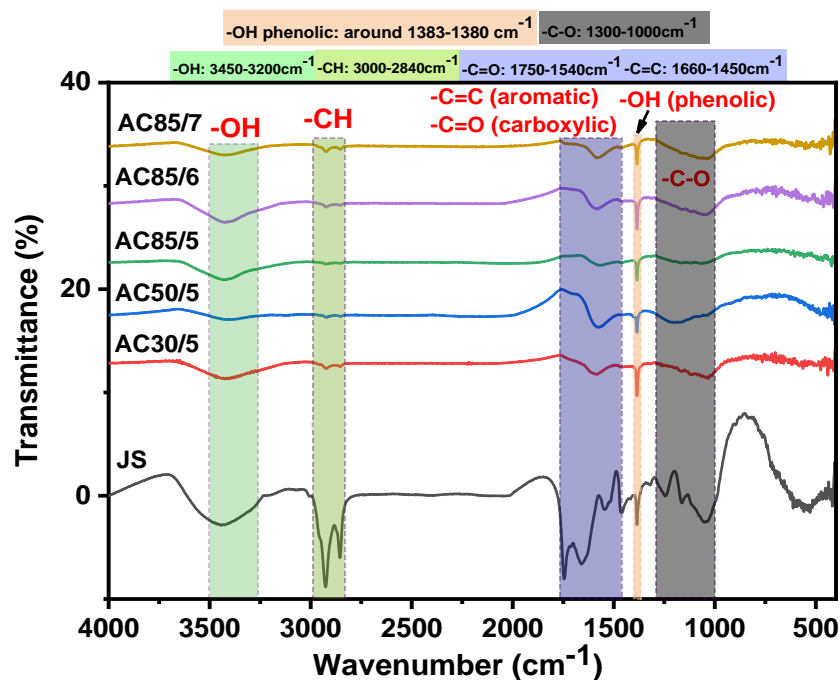
Figure 2. FTIR spectra of the prepared Acs.

3.4. SEM Analysis

Figure 3 illustrates the micrographs of the JS and the prepared activated carbons. Figure 3A depicts the surface of the JS, which seems compact, uneven and devoid of any pore structure. Comparing micrographs of the three activated carbons AC30/5, AC50/5 and AC85/5 showed a non-developed porous structure of the activated carbon chemically activated with 30% phosphoric acid (Figure 3B). This can be attributed to the inadequate influence of low phosphoric acid concentration (30%) on the JS morphology to create a porous activated carbon. On the other hand, Figure 3C,D displays the development of irregular particles of different sizes, featuring pores, cavities and cracks on their surfaces. The pores and cavities observed on the surfaces of carbons were created as a result of the activating agent's evaporation during carbonization [60]. A significant amount of volatile matter was also removed during the chemical activation using phosphoric acid, resulting in the opening and the growth of pores on the surface of the adsorbents and to the enlargement of the pre-existing pores [70]. Under various carbonization conditions (Figure 3D–F), the surface texture of the activated carbons prepared at 500 and 600 °C showed significantly pronounced cavities and cracks on their surfaces. With increasing temperature, the microporous structure deteriorated, causing an apparent reduction in porosity with a smaller internal surface (Figure 3F).
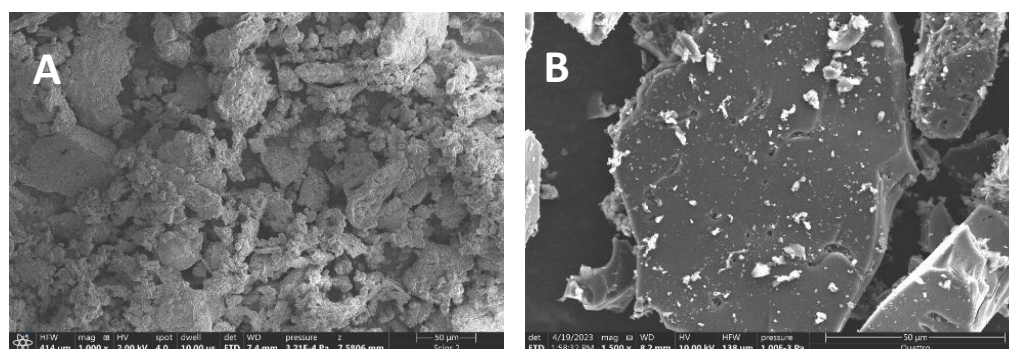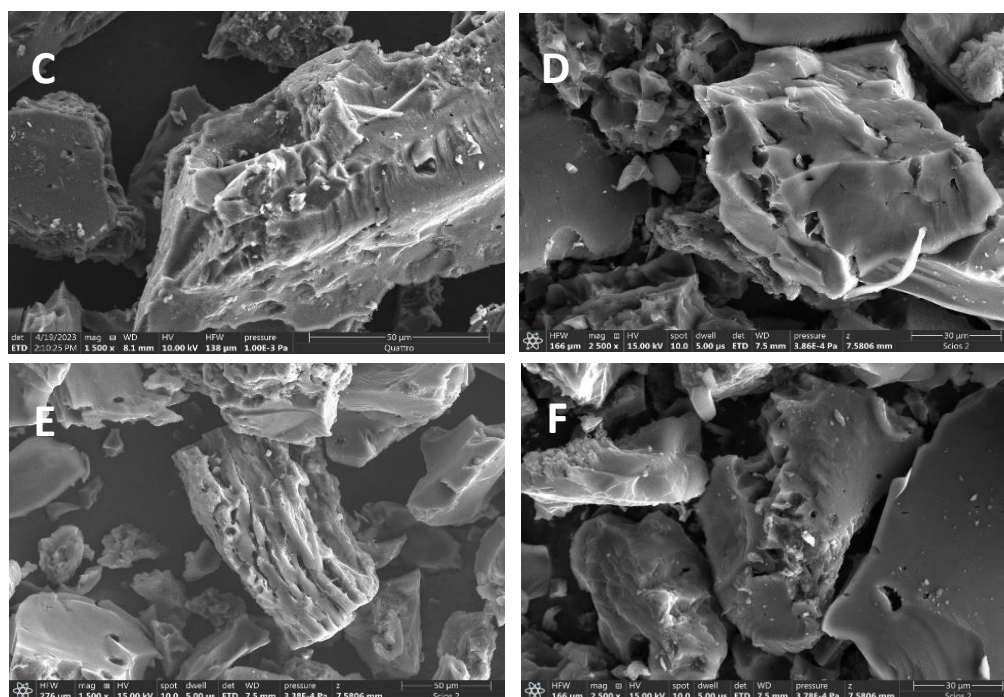

Figure 3. *Cont.*

Figure 3. SEM micrographs of (**A**) JS × 1000, (**B**) AC30/5 × 1500, (**C**) AC50/5 × 1500, (**D**) AC85/5 × 2500, (**E**) AC85/6 × 1500 and (**F**) AC85/7 × 2500.

3.5. XRD Analysis

Figure 4 illustrates the XRD plots of the jujube stones (JS) and the five prepared activated carbons. As is typical of amorphous materials, none of the patterns displayed sharp and distinguishable peaks [14]. The peak observed in JS was around 21.5° revealing an amorphous carbon structure [71]. The activated carbons showed two broad peaks at the 2θ range 20–30° (with maximum intensity at around 25°) and at 2θ range 40–50° (with maximum intensity at around 43°) [72,73]. These two peaks observed at around 25 and 43° were attributed to the reflection of the (0 0 2) and (1 0 0) planes, and can be linked to the presence of graphite [72] and dehydrated hemicellulose [74], respectively. The sharp peaks observed at around 72.5° may reveal the presence of a graphitic crystalline structure in the JS and the ACs [75]; this structure may be related to the hexagonal carbon phase (1 0 19). The same peak has also been found in the XRD patterns of ACs derived from whole bagasse under various conditions [76], but was not identified. The almost complete disappearance of this peak in the spectrum of AC85/7 is presumably due to the thermal stabilization of graphite and the destruction of the crystalline structure at higher activation temperatures.

The characterization results show that using pure phosphoric acid (85 wt%) enabled greater JS activation, and its carbonization at 600 °C produced an excellent activated carbon with better adsorption properties. As a result, the AC85/6 was chosen for the Mustard- and Violet-effluent decolorization.

The activated carbons investigated in this research were produced through the chemical activation of jujube stones using phosphoric acid. The utilization of phosphoric acid (H_3PO_4) as an activating agent presents a myriad of notable advantages within the activated carbon preparation process. Beyond its favorable attributes for the decomposition of ligno-cellulosic precursors at relatively low activation temperatures and its ability to mitigate activation equipment corrosion, phosphoric acid imparts an array of other pivotal benefits. Its utilization stands out due to its low cost and environmentally conscientious profile. In comparison to other costlier or potentially hazardous activation agents, phosphoric acid provides an economical and enduring solution for the production of high-quality activated carbons [14].
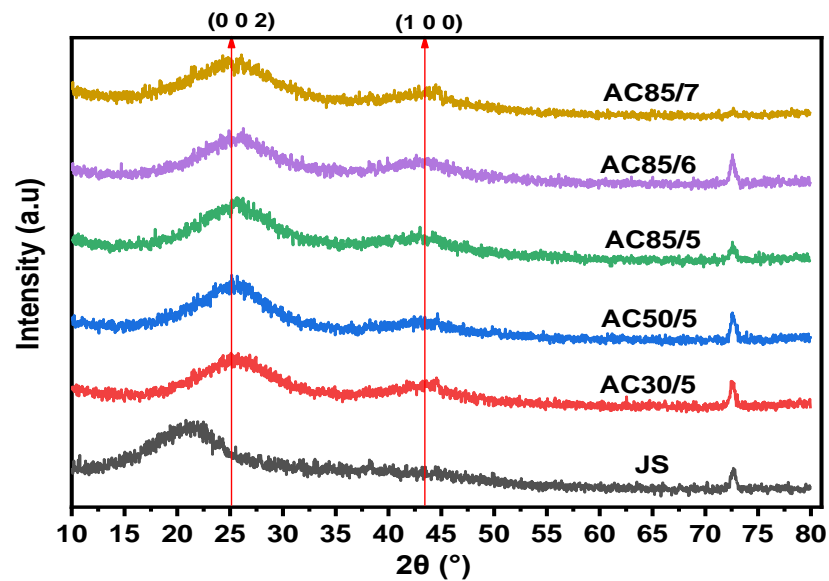
Figure 4. X-ray diffraction diagrams of the JS and the ACs.

The reliability of H_3PO_4 as an activating agent has been substantiated through a comparison of the performance of the activated carbon produced in this investigation with other activated carbons documented in the literature, which were prepared using alternative activating agents and used for the treatment of industrial effluents (Table 3).

Table 3. Comparison of the H_3PO_4 performances with other activating agents.

Adsorbent	Activating Agent	Preparation Conditions	Methylene Blue Index (mg/g)	S_{MB} (m²/g)	Iodine Number (mg/g)	Reference
Pine sawdust (PS)-based activated carbon	$ZnCl_2$	1.5/1 Imp. ratio (w/w)/carbonization at 400 °C/2 h	300	/	/	[77]
Rose seed (RS)-based activated carbon	$ZnCl_2$	1.5/1 Imp. ratio (w/w); carbonization at 500 °C/3 h	297	/	/	[77]
Cornel seed (CS)-based activated carbon	$ZnCl_2$	1.5/1 Imp. ratio (w/w); carbonization at 500 °C/2 h	299		/	[77]
Jujube stone-based activated carbon	KOH	1/2 Imp. ratio (w/w); carbonization at 700 °C/3 h	299.02	/	1358.05	[62]
Jujube stone-based activated carbon	H_3PO_4	1/1 Imp. ratio (w/w); carbonization at 600 °C/1 h	387.61	948.84	867.54	This study
Acacia erioloba seed pods-based activated carbon (<50 μm)	H_2SO_4		/	10.47	528 ± 2.9	[78]
Acacia erioloba seed pods-based activated carbon (<75 μm)	H_2SO_4	25 g + 150 mL 10% H_2SO_4; carbonization at 600 °C/1 h	/	10.34	638 ± 3.1	[78]
Acacia erioloba seed pods-based activated carbon (<100 μm)	H_2SO_4		/	10.31	554 ± 2.4	[78]

3.6. Textile Effluents Treatment

The aim of this section is to assess the effectiveness of AC85/6 activated carbon as an adsorbent for the treatment of dye-laden textile effluents. Two effluents were examined: Mustard effluent and Violet effluent. Table 4 summarizes their characteristics.

Table 4. Physico-chemical characteristics of the untreated Mustard and Violet effluents.

Parameter	Mustard Effluent	Violet Effluent	Algerian Standard * N° 06-141, 2006	Textile Factory's Internal Specifications	World Health Organization (WHO) Standard [57]
Temperature (°C)	17.95	17.31	35	<30	/
pH	9.19	9.24	6.0–9.0	6.5–8.5	6.5–8.5
turbidity (FTU)	7.52	8.09	-	-	-
COD (mg O_2/L)	302.72	230.68	300	120	<90
BOD (mg O_2/L)	80.00	60.00	200	40	<30
COD/BOD	3.78	3.84	-	-	-
suspended solids (mg/L)	63.00	45.00	40	40	<20
Total dissolved solids (mg/L)	1864.00	1397.00	-	-	-
Total solid (mg/L)	1927.00	1442.00	-	-	-

* Tolerance to limit values old installations.

All investigations were replicated three times to confirm the results.

Effluent guidelines and standards govern the direct release of effluents into surface waters. The characteristics of the two studied effluents were compared with the Algerian standard, the limit values tolerated by the WHO, and the internal requirements of the textile factory. The physical and chemical parameters of both effluents exceed WHO tolerances as well as the factory's internal requirements. The Algerian standard is less stringent regarding BOD, COD and pH for older installations. Both effluents exhibited highly basic pH values and substantial levels of BOD and COD before treatment. It should be observed that the COD/BOD ratios for both effluents were higher than three, indicating that these effluents are difficult to biodegrade [57] and therefore require physical and/or chemical treatments before being discharged into the environment, which justifies the choice of the adsorption on activated carbon in this work as an effective physical method for the treatment of colored textile wastewater.

To determine the maximum wavelength (λ_{max}) of the dyes present in the two effluents, a UV–visible spectrophotometer (Agilent Technologies, Cary 60) was utilized. The λ_{max} in the visible light region was found to be 420 nm for the Mustard effluent and 540 nm for the Violet effluent (Figure S1).

The effectiveness of AC85/6 in decolorizing the investigated wastewaters was evaluated by calculating the percentage of decolorization (% decolorization) given by the following equation [79,80].

$$Decolorization~(\%) = 100 \times \frac{Abs_0 - Abs_f}{Abs_0} \tag{1}$$

where Abs_0 is the absorbance at λ_{max} before adsorption (initial absorbance) and Abs_f is the absorbance at λ_{max} after adsorption (final absorbance).

The effect of adsorbate/adsorbent contact time and AC85/6 dosage were studied at effluent pH and ambient temperature.

3.6.1. Effect of Contact Time

The contact time is a critical parameter for controlling the efficiency of the adsorption phenomena and estimating the time required to attain adsorption equilibrium. The effect of contact time on Mustard- and Violet-effluent adsorption was investigated using AC85/6 adsorbent at contact durations ranging from 5–180 min with an adsorbent dosage of 1 g/L at ambient temperature and at effluent pH. The accompanying figure (Figure 5) depict the curves corresponding to the adsorption kinetics of the two effluents on the AC85/6.

The graphs represent the evolution of decolorization by AC85/6 of Mustard and Violet effluents as a function of time (5–180 min). Adsorption kinetics were found to be fast in both graphs during the first minutes of adsorbent/adsorbate interaction. This can possibly be attributed to ready availability of adsorption sites [81]. The repulsive forces that occur between the dye molecules adsorbed on the adsorbent surface and the solution phase make filling the remaining unoccupied sites more challenging [24]. Finally, a plateau

was observed matching the liquid−solid equilibrium. For both effluents, equilibrium was reached after about 60 min of contact.
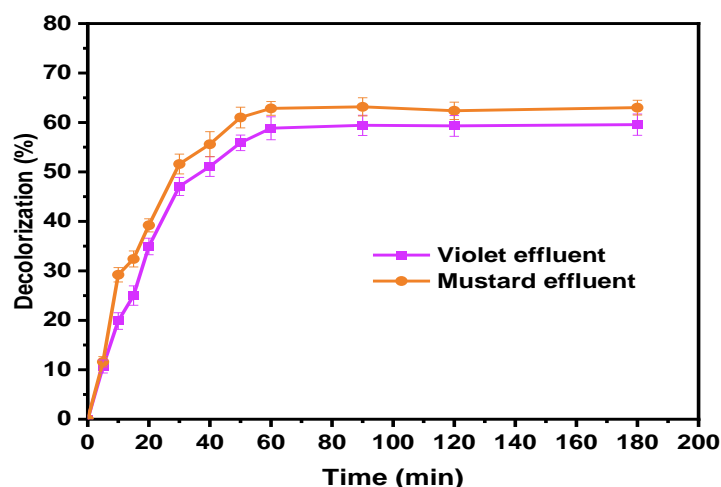

Figure 5. Effect of contact time on the decolorization percentage of the Mustard and Violet effluent on AC85/6 (pH of the effluent, ambient temperature (22 °C ± 5), adsorbent dosage = 1 g/L).

3.6.2. Effect of Adsorbent Dosage

The decolorization of Mustard and Violet textile effluent was tested using AC85/6 dosages ranging from 0.1 to 6 g/L.

Figure 6 depicts the effect of activated carbon dosage on Mustard- and Violet-effluents treatment, demonstrating that decolorization rates increased when increasing the adsorbent dosage. This tendency can be associated with an increase in AC85/6 active sites with increasing dosage, resulting in enhanced adsorption [82]. The maximum achieved decolorization percentages for both effluents were 81.03% for the Violet effluent and 84.65% for the Mustard, reached with an adsorbent dosage of 4 g/L. Above this dosage, no discernible difference in dye removal was observed and the decolorization rate remained nearly constant even when more active sites were available. Consequently, using higher doses simply results in inefficient expenditure and adsorbent mass loss [23]. In conclusion, the AC85/6 dose of 4 g/L was identified as the optimal dosage.
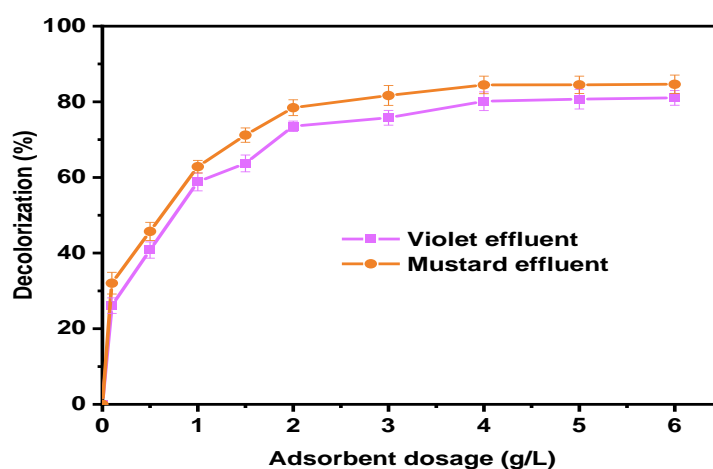

Figure 6. Effect of AC85/6 dosage on the treatment percentage of the Mustard and Violet effluent (pH of the effluent, ambient temperature (22 °C ± 5), contact time = 180 min).

3.6.3. Physico-Chemical Characteristics of Wastewater before and after Treatment

The results of the physico-chemical analysis of the two effluents before and after treatment with AC85/6, as well as the limit values for textile effluents according to Algerian regulation, WHO directives and the textile factory requirements, are shown in Table 5.

Table 5. Physico-chemical characteristics of wastewaters before and after treatment.

Parameter	Mustard Effluent		Violet Effluent	
	before Treatment	after Treatment with AC85/6	before Treatment	after Treatment with AC85/6
Temperature (°C)	17.95	16.59 ± 0.54	17.31	16.10 ± 1.01
pH	9.19	7.38 ± 0.21	9.24	7.44 ± 0.43
turbidity (FTU)	7.52	0.22 ± 0.07	8.09	0.51 ± 0.13
turbidity removal (%)	/	97.07 ± 0.93	/	93.70 ± 1.61
COD (mg O_2/L)	302.72	96.04 ± 2.57	230.68	80.51 ± 3.61
COD removal (%)	/	68.27 ± 0.85	/	65.10 ± 1.56
BOD (mg O_2/L)	80.00	40.00	60.00	20.00
BOD removal (%)	/	50.00	/	66.67
suspended solids (mg/L)	63.00	0.26 ± 0.04	45.00	0.43 ± 0.09
suspended solids removal (%)	/	99.59 ± 0.06	/	99.04 ± 0.20
Total dissolved solids (mg/L)	1864.00	767.00 ± 7.00	1397.00	635.00 ± 5.00
Total dissolved solids removal (%)	/	58.85 ± 0.38	/	54.55 ± 0.36
Total solid (mg/L)	1927.00	767.26 ± 7.04	1442.00	635.43 ± 5.09
Total solids removal (%)	/	60.18 ± 0.37	/	55.93 ± 0.25

Tolerance to limit values for old installations.

The temperature of both effluents was around 17–18 °C, which is below the recommended value of standard levels (shown in Table 4). The pH values of the two collected samples were highly basic and above the permissible limits. This may be linked to the quality of the dyes used and the addition of carbonates and salts in the dyeing process [83]. Many other researchers have also confirmed the alkaline nature of wastewater from the textile industry [57,79,84,85]. Activated carbon treatment reduced the pH of both wastewaters, bringing the resulting values within the permissible range. The amount of oxygen required by micro-organisms to oxidize organic matter is measured using BOD (biochemical oxygen demand). The amount of dissolved oxygen (DO) in watercourses is directly affected by BOD. High levels of BOD reduce DO levels, leading to disruption, asphyxiation and death of aquatic organisms [83]. Increased COD, on the other hand, can be linked to increased addition of organic and inorganic pollutants used during the fabric manufacturing process, and to the presence of physiologically resistant organic chemicals [83,86]. The BOD and COD values of the Mustard effluent were slightly higher than those of the Violet effluent before treatment. After treatment, BOD and COD reduction percentages for Mustard effluent were as good as for Violet effluent. The WHO limits for BOD and COD are quite stringent, with no more than 30 mg/L and 90 mg/L allowed, respectively. Total dissolved solids (TDS) mainly consist of carbonates, bicarbonates, chlorides, phosphates and nitrates of calcium, magnesium, potassium and manganese, as well as organic matter salts and other particles. The intense coloration could be associated to the high amount of TDS [86]. Treatment with AC85/6 resulted in 58.85% and 54.55% TDS removal from the Mustard and Violet effluents, respectively, and almost total removal of suspended solids.

Color changes in Mustard and Violet effluents after adsorption on AC85/6 are illustrated in Figure 7. The absorbances of untreated wastewater effluents are also shown for comparison. It can be seen that absorbance values decreased significantly in the treated samples compared with the untreated samples. Absorbances decreased from 0.272 to 0.051 for the Violet effluent and from 0.250 to 0.038 for the Mustard effluent, with decolorization percentages of 81.03 and 84.65%, respectively, confirming the effectiveness of prepared activated carbon AC85/6 in the treatment of textile effluents loaded with various dyes. Similarly, Baral et al. [87] studied the light-assisted decolorization of rhodamine B dye (RhB).

Decolorization was assessed on the basis of the decrease in intensity of the absorption band positioned at 554 nm. The results showed total decolorization of RhB in 10 min.
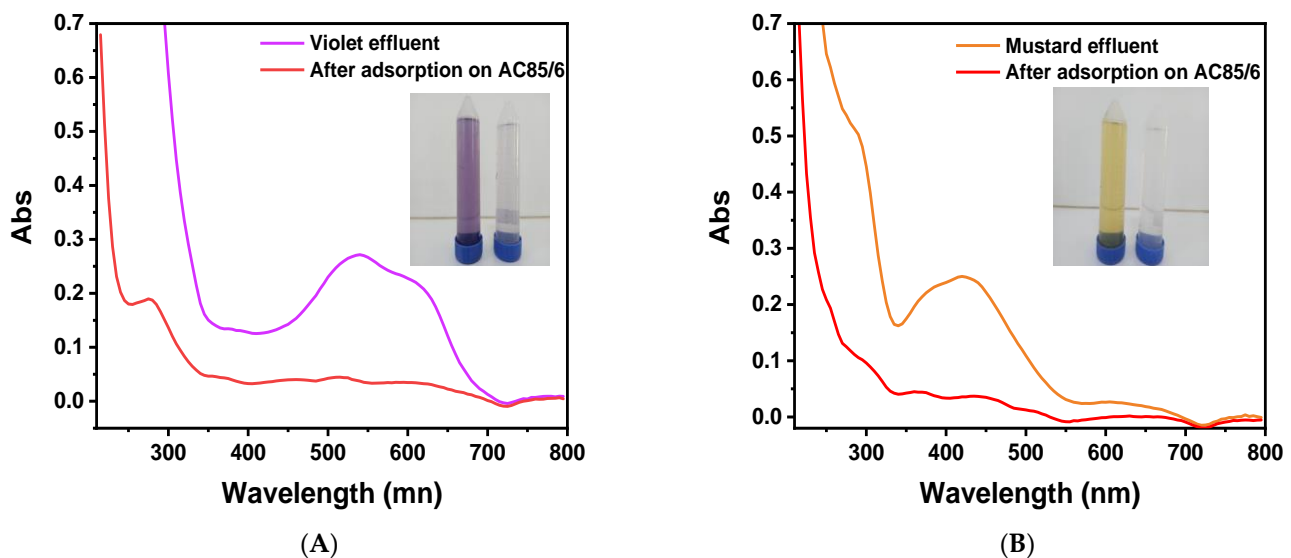

(**A**)

(**B**)

Figure 7. UV–vis spectra for (**A**) the Violet-effluent adsorption onto the AC85/6 and (**B**) Mustard-effluent adsorption onto the AC85/6.

The COD removal efficiencies achieved on the prepared activated carbon for Mustard and Violet effluent were 84.65% and 81.03%, respectively, higher than those obtained by some other activated carbons and adsorbents listed in Table 6 confirming its performance as an effective alternative for treating industrial wastewater.

Table 6. Comparison COD removal efficiencies by various adsorbents.

Adsorbent	Adsorbent Dosage (g/L)	COD before Treatment (mg O_2/L)	COD Removal (%)	Reference
Bamboo-based activated carbon	3	251.65	75.21	[88]
wheat straw activated carbon	2.045	1313	90.92	[46]
Sphagnum moss peat	20	665	44.128	[51]
Sulfuric acid activated bentonite	2	569 $\pm$ 23	76.5	[89]
Jujube stone-based activated carbon	4	302.72	84.65	This study
	4	230.68	81.03	This study
Coal fly ash	40	665	61.11	[90]
Cypress cones activated carbon	2	865	19	[91]
Sugarcane bagasse	10	347.8	55.07	[92]
Coir pith activated carbon (CPC)	5	528	46.5	[93]
Granular coir pith carbon (GCPC)	5	528	35	[93]

4. Conclusions

In this work, activated carbons were prepared by chemical activation of jujube stones using phosphoric acid. Boehm analysis and FTIR characterization of the prepared ACs revealed the presence of several functional groups responsible for adsorption. Scanning electron microscopy showed the presence of cavities, more or less homogeneous, on the surfaces of the prepared activated carbons, demonstrating different levels of surface devel-

opment and morphology. XRD analysis revealed amorphous structures of the prepared ACs. The physicochemical analysis of the quality of the wastewater recovered from the textile factory revealed that they represent a significant source of pollution and are detrimental to the environment if released directly without treatment. Both collected effluents were characterized by basic pH values and high levels of BOD, COD, turbidity, suspended solids and dissolved solids. Their treatment by adsorption on the AC85/6 gave good results. A contact time of 60 min and an AC85/6 dosage of 4 g/L were sufficient for maximum decolorization of both effluents. After AC85/6 treatment, the results showed a significant reduction in the values of the physiochemical investigated parameters. The limits for textile discharges fixed by the Algerian standard, as well as the internal requirements of the textile factory were respected. The BOD and COD values of the Mustard effluent were slightly higher than the very strict WHO guidelines. The present research study demonstrated the effectiveness of prepared activated carbons as low-cost adsorbents for the treatment of dyeing effluents.

Author Contributions: Conceptualization, N.B., K.B., N.H., H.B. and L.M.; methodology, N.B., A.Z., H.B. and L.M.; software, N.B., F.A. and A.Z.; validation, H.B., A.A., L.B. and L.M.; formal analysis, A.A., H.B. and L.M.; investigation, N.B.; resources, L.M., A.Z. and F.A.; data curation, N.B., A.M., K.B. and L.M.; writing—original draft preparation, N.B.; writing—review and editing, A.M., N.H.,H.B. and L.M.; visualization, N.B., L.B., H.B., L.M. and A.A.; supervision, L.M., H.B., A.Z. and A.A.; project administration, L.M. and A.A. and funding acquisition, L.M. and A.A. All authors have read and agreed to the published version of the manuscript.

Data Availability Statement: Not applicable.

Conflicts of Interest: The authors declare no conflict of interest.

References

1. Mia, R.; Selim, M.; Shamim, A.; Chowdhury, M.; Sultana, S.; Armin, M.; Hossain, M.; Akter, R.; Dey, S.; Naznin, H. Review on various types of pollution problem in textile dyeing & printing industries of Bangladesh and recommandation for mitigation. *J. Text. Eng. Fash. Technol.* **2019**, *5*, 220–226.
2. Bhagat, S.K.; Pilario, K.E.; Emmanuel, B.O.; Tiyasha, T.; Yaqub, M.; Onu, C.E.; Pyrgaki, K.; Falah, M.W.; Jawad, A.H.; Yaseen, D.A. Comprehensive review on machine learning methodologies for modeling dye removal processes in wastewater. *J. Clean. Prod.* **2023**, *385*, 135522.
3. Solayman, H.; Hossen, M.A.; Abd Aziz, A.; Yahya, N.Y.; Hon, L.K.; Ching, S.L.; Monir, M.U.; Zoh, K.-D. Performance evaluation of dye wastewater treatment technologies: A review. *J. Environ. Chem. Eng.* **2023**, *11*, 109610.
4. Zidane, F.; Kaba, N.; Bensaid, J.; Blais, J.F.; Drogui, P.; Rhazzar, A.; Lekhlif, B.; Benabdenbi, B. Contribution ā la dépollution d'un rejet textile par adsorption sur un coagulant ā base du mélange fer/aluminium préparé par électrocoagulation. *Int. J. Biol. Chem. Sci.* **2011**, *5*, 2094–2102. [CrossRef]
5. Hassan, M.M.; Saifullah, K. Ultrasound-assisted sustainable and energy efficient pre-treatments, dyeing, and finishing of textiles–A comprehensive review. *Sustain. Chem. Pharm.* **2023**, *33*, 101109. [CrossRef]
6. Donkadokula, N.Y.; Kola, A.K.; Naz, I.; Saroj, D. A review on advanced physico-chemical and biological textile dye wastewater treatment techniques. *Rev. Environ. Sci. Bio/Technol.* **2020**, *19*, 543–560. [CrossRef]
7. Reddy, S.S.; Kotaiah, B.; Reddy, N.S.P. Color pollution control in textile dyeing industry effluents using tannery sludge derived activated carbon. *Bull. Chem. Soc. Ethiop.* **2008**, *22*, 369–378.
8. Hassan, M.M.; Carr, C.M. A critical review on recent advancements of the removal of reactive dyes from dyehouse effluent by ion-exchange adsorbents. *Chemosphere* **2018**, *209*, 201–219. [CrossRef]
9. Afroze, S.; Sen, T.K. A review on heavy metal ions and dye adsorption from water by agricultural solid waste adsorbents. *Water Air Soil Pollut.* **2018**, *229*, 225.

10. Al-Tohamy, R.; Ali, S.S.; Li, F.; Okasha, K.M.; Mahmoud, Y.A.-G.; Elsamahy, T.; Jiao, H.; Fu, Y.; Sun, J. A critical review on the treatment of dye-containing wastewater: Ecotoxicological and health concerns of textile dyes and possible remediation approaches for environmental safety. *Ecotoxicol. Environ. Saf.* **2022**, *231*, 113160. [CrossRef]

11. Arslan, S.; Eyvaz, M.; Gürbulak, E.; Yüksel, E. A review of state-of-the-art technologies in dye-containing wastewater treatment–the textile industry case. In *Textile Wastewater Treatment*; IntechOpen: London, UK, 2016.

12. Samsami, S.; Mohamadizaniani, M.; Sarrafzadeh, M.-H.; Rene, E.R.; Firoozbahr, M. Recent advances in the treatment of dye-containing wastewater from textile industries: Overview and perspectives. *Process Saf. Environ. Prot.* **2020**, *143*, 138–163. [CrossRef]

13. Su, M.; Li, H.; He, X.; Xu, Z. Significant enhancement of pesticide and organic dyes degradation by ion-exchange within a metal–organic framework. *Polyhedron* **2022**, *215*, 115651. [CrossRef]

14. Bouchelkia, N.; Tahraoui, H.; Amrane, A.; Belkacemi, H.; Bollinger, J.-C.; Bouzaza, A.; Zoukel, A.; Zhang, J.; Mouni, L. Jujube stones based highly efficient activated carbon for methylene blue adsorption: Kinetics and isotherms modeling, thermodynamics and mechanism study, optimization via response surface methodology and machine learning approaches. *Process Saf. Environ. Prot.* **2023**, *170*, 513–535. [CrossRef]

15. Rambabu, K.; Bharath, G.; Monash, P.; Velu, S.; Banat, F.; Naushad, M.; Arthanareeswaran, G.; Show, P.L. Effective treatment of dye polluted wastewater using nanoporous $CaCl_2$ modified polyethersulfone membrane. *Process Saf. Environ. Prot.* **2019**, *124*, 266–278. [CrossRef]

16. Bangari, R.S.; Yadav, A.; Bharadwaj, J.; Sinha, N. Boron nitride nanosheets incorporated polyvinylidene fluoride mixed matrix membranes for removal of methylene blue from aqueous stream. *J. Environ. Chem. Eng.* **2022**, *10*, 107052. [CrossRef]

17. Hadadi, A.; Imessaoudene, A.; Bollinger, J.-C.; Cheikh, S.; Assadi, A.A.; Amrane, A.; Kebir, M.; Mouni, L. Parametrical Study for the Effective Removal of Mordant Black 11 from Synthetic Solutions: Moringa oleifera Seeds' Extracts Versus Alum. *Water* **2022**, *14*, 4109. [CrossRef]

18. Bilińska, L.; Gmurek, M.; Ledakowicz, S. Textile wastewater treatment by AOPs for brine reuse. *Process Saf. Environ. Prot.* **2017**, *109*, 420–428. [CrossRef]

19. Wang, Y.; Sun, T.; Tong, L.; Gao, Y.; Zhang, H.; Zhang, Y.; Wang, Z.; Zhu, S. Non-free Fe dominated PMS activation for enhancing electro-Fenton efficiency in neutral wastewater. *J. Electroanal. Chem.* **2023**, *928*, 117062. [CrossRef]

20. Yin, C.; Ma, J.; Qiu, J.; Liu, R.; Ba, L. Mass-producible low-cost flexible electronic fabrics for azo dye wastewater treatment by electrocoagulation. *Chin. J. Chem. Eng.* **2023**, *59*, 222–230. [CrossRef]

21. Kalsoom, U.; Khalid, N.; Ibrahim, A.; Ashraf, S.S.; Bhatti, H.N.; Ahsan, Z.; Zdarta, J.; Bilal, M. Biocatalytic degradation of reactive blue 221 and direct blue 297 dyes by horseradish peroxidase immobilized on iron oxide nanoparticles with improved kinetic and thermodynamic characteristics. *Chemosphere* **2023**, *312*, 137095. [CrossRef]

22. Amin, S.; Rastogi, R.P.; Chaubey, M.G.; Jain, K.; Divecha, J.; Desai, C.; Madamwar, D. Degradation and toxicity analysis of a reactive textile diazo dye-Direct Red 81 by newly isolated Bacillus sp. DMS2. *Front. Microbiol.* **2020**, *11*, 576680. [CrossRef] [PubMed]

23. Cheikh, S.; Imessaoudene, A.; Bollinger, J.-C.; Hadadi, A.; Manseri, A.; Bouzaza, A.; Assadi, A.; Amrane, A.; Zamouche, M.; El Jery, A. Complete Elimination of the Ciprofloxacin Antibiotic from Water by the combination of Adsorption–Photocatalysis Process using Natural Hydroxyapatite and TiO_2. *Catalysts* **2023**, *13*, 336. [CrossRef]

24. Imessaoudene, A.; Cheikh, S.; Bollinger, J.-C.; Belkhiri, L.; Tiri, A.; Bouzaza, A.; El Jery, A.; Assadi, A.; Amrane, A.; Mouni, L. Zeolite Waste Characterization and Use as Low-Cost, Ecofriendly, and Sustainable Material for Malachite Green and Methylene Blue Dyes Removal: Box–Behnken Design, Kinetics, and Thermodynamics. *Appl. Sci.* **2022**, *12*, 7587. [CrossRef]

25. Ileri, B.; Dogu, I. Sono–degradation of Reactive Blue 19 in aqueous solution and synthetic textile industry wastewater by nanoscale zero–valent aluminum. *J. Environ. Manag.* **2022**, *303*, 114200. [CrossRef] [PubMed]

26. Khan, M.; Ali, S.W.; Shahadat, M.; Sagadevan, S. Applications of polyaniline-impregnated silica gel-based nanocomposites in wastewater treatment as an efficient adsorbent of some important organic dyes. *Green Process. Synth.* **2022**, *11*, 617–630. [CrossRef]

27. Hadadi, A.; Imessaoudene, A.; Bollinger, J.-C.; Cheikh, S.; Manseri, A.; Mouni, L. Dual Valorization of Potato Peel (Solanum tuberosum) as a Versatile and Sustainable Agricultural Waste in Both Bioflocculation of Eriochrome Black T and Biosorption of Methylene Blue. *J. Polym. Environ.* **2023**, *31*, 2983–2998. [CrossRef]

28. Bouchelkia, N.; Mouni, L.; Belkhiri, L.; Bouzaza, A.; Bollinger, J.-C.; Madani, K.; Dahmoune, F. Removal of lead (II) from water using activated carbon developed from jujube stones, a low-cost sorbent. *Sep. Sci. Technol.* **2016**, *51*, 1645–1653. [CrossRef]

29. Chedri Mammar, A.; Mouni, L.; Bollinger, J.-C.; Belkhiri, L.; Bouzaza, A.; Assadi, A.A.; Belkacemi, H. Modeling and optimization of process parameters in elucidating the adsorption mechanism of Gallic acid on activated carbon prepared from date stones. *Sep. Sci. Technol.* **2020**, *55*, 3113–3125. [CrossRef]

30. Kausar, A.; Iqbal, M.; Javed, A.; Aftab, K.; Bhatti, H.N.; Nouren, S. Dyes adsorption using clay and modified clay: A review. *J. Mol. Liq.* **2018**, *256*, 395–407. [CrossRef]

31. Karimi, S.; Yaraki, M.T.; Karri, R.R. A comprehensive review of the adsorption mechanisms and factors influencing the adsorption process from the perspective of bioethanol dehydration. *Renew. Sustain. Energy Rev.* **2019**, *107*, 535–553. [CrossRef]

32. Patel, H. Fixed-bed column adsorption study: A comprehensive review. *Appl. Water Sci.* **2019**, *9*, 45. [CrossRef]

33. Daniel, L.S.; Rahman, A.; Hamushembe, M.N.; Kapolo, P.; Uahengo, V.; Jonnalagadda, S.B. The production of activated carbon from Acacia erioloba seedpods via phosphoric acid activation method for the removal of methylene blue from water. *Bioresour. Technol. Rep.* **2023**, *23*, 101568. [CrossRef]

34. Dias, J.M.; Alvim-Ferraz, M.C.; Almeida, M.F.; Rivera-Utrilla, J.; Sánchez-Polo, M. Waste materials for activated carbon preparation and its use in aqueous-phase treatment: A review. *J. Environ. Manag.* **2007**, *85*, 833–846. [CrossRef] [PubMed]

35. Regti, A.; El Kassimi, A.; Laamari, M.R.; El Haddad, M. Competitive adsorption and optimization of binary mixture of textile dyes: A factorial design analysis. *J. Assoc. Arab. Univ. Basic Appl. Sci.* **2017**, *24*, 1–9. [CrossRef]

36. Erto, A.; Chianese, S.; Lancia, A.; Musmarra, D. On the mechanism of benzene and toluene adsorption in single-compound and binary systems: Energetic interactions and competitive effects. *Desalination Water Treat.* **2017**, *86*, 259–265. [CrossRef]

37. El Gamal, M.; Mousa, H.A.; El-Naas, M.H.; Zacharia, R.; Judd, S. Bio-regeneration of activated carbon: A comprehensive review. *Sep. Purif. Technol.* **2018**, *197*, 345–359. [CrossRef]

38. Akkari, I.; Graba, Z.; Bezzi, N.; Kaci, M.M.; Merzeg, F.A.; Bait, N.; Ferhati, A.; Dotto, G.L.; Benguerba, Y. Effective removal of cationic dye on activated carbon made from cactus fruit peels: A combined experimental and theoretical study. *Environ. Sci. Pollut. Res.* **2023**, *30*, 3027–3044. [CrossRef]

39. Bayomie, O.S.; Kandeel, H.; Shoeib, T.; Yang, H.; Youssef, N.; El-Sayed, M.M. Novel approach for effective removal of methylene blue dye from water using fava bean peel waste. *Sci. Rep.* **2020**, *10*, 7824. [CrossRef]

40. Ramutshatsha-Makhwedzha, D.; Mavhungu, A.; Moropeng, M.L.; Mbaya, R. Activated carbon derived from waste orange and lemon peels for the adsorption of methyl orange and methylene blue dyes from wastewater. *Heliyon* **2022**, *8*, e09930. [CrossRef]

41. Raji, Y.; Nadi, A.; Mechnou, I.; Saadouni, M.; Cherkaoui, O.; Zyade, S. High adsorption capacities of crystal violet dye by low-cost activated carbon prepared from Moroccan Moringa oleifera wastes: Characterization, adsorption and mechanism study. *Diam. Relat. Mater.* **2023**, *135*, 109834. [CrossRef]

42. Amibo, T.A.; Beyn, S.M.; Bayu, A.B.; Kabeta, W.F. Optimization and Modeling of Cr (VI) Removal from Tannery Wastewater onto Activated Carbon Prepared from Coffee Husk and Sulfuric Acid (H_2SO_4) as Activating Agent by Using Central Composite Design (CCD). *J. Environ. Public Health* **2023**, *2023*, 5663261.

43. Milanković, V.; Tasić, T.; Pejčić, M.; Pašti, I.; Lazarević-Pašti, T. Spent Coffee Grounds as an Adsorbent for Malathion and Chlorpyrifos—Kinetics, Thermodynamics, and Eco-Neurotoxicity. *Foods* **2023**, *12*, 2397. [CrossRef]

44. Yusop, M.F.M.; Khan, M.N.N.; Zakaria, R.; Abdullah, A.Z.; Ahmad, M.A. Mass transfer simulation on remazol brilliant blue R dye adsorption by optimized teak wood Based activated carbon. *Arab. J. Chem.* **2023**, *16*, 104780. [CrossRef]

45. Yusop, M.F.M.; Jaya, M.A.T.; Idris, I.; Abdullah, A.Z.; Ahmad, M.A. Optimization and mass transfer simulation of remazol brilliant blue R dye adsorption onto meranti wood based activated carbon. *Arab. J. Chem.* **2023**, *16*, 104683. [CrossRef]

46. Agarwal, S.; Singh, A.P.; Mathur, S. Removal of COD and color from textile industrial wastewater using wheat straw activated carbon: An application of response surface and artificial neural network modeling. *Environ. Sci. Pollut. Res.* **2023**, *30*, 41073–41094. [CrossRef] [PubMed]

47. Khan, T.A.; Nouman, M.; Dua, D.; Khan, S.A.; Alharthi, S.S. Adsorptive scavenging of cationic dyes from aquatic phase by H_3PO_4 activated Indian jujube (*Ziziphus mauritiana*) seeds based activated carbon: Isotherm, kinetics, and thermodynamic study. *J. Saudi Chem. Soc.* **2022**, *26*, 101417. [CrossRef]

48. Hung, N.V.; Nguyet, B.T.M.; Nghi, N.H.; Thanh, N.M.; Quyen, N.D.V.; Nguyen, V.T.; Nhiem, D.N.; Khieu, D.Q. Highly effective adsorption of organic dyes from aqueous solutions on longan seed-derived activated carbon. *Environ. Eng. Res.* **2022**, *28*, 220116. [CrossRef]

49. Wickramaarachchi, W.K.P.; Minakshi, M.; Gao, X.; Dabare, R.; Wong, K.W. Hierarchical porous carbon from mango seed husk for electro-chemical energy storage. *Chem. Eng. J. Adv.* **2021**, *8*, 100158. [CrossRef]

50. Wickramaarachchi, K.; Minakshi, M.; Aravindh, S.A.; Dabare, R.; Gao, X.; Jiang, Z.-T.; Wong, K.W. Repurposing N-doped grape marc for the fabrication of supercapacitors with theoretical and machine learning models. *Nanomaterials* **2022**, *12*, 1847. [CrossRef]

51. Zaharia, C. Application of a physico-chemical treatment based on adsorption for industrial effluents. A case study. In Proceedings of the 16th International Conference–Modern Technologies, Quality and Innovation–ModTech, Sinaia, Romania, 24–26 May 2012; pp. 1069–1072.

52. Ahmed, M.J.; Dhedan, S.K. Equilibrium isotherms and kinetics modeling of methylene blue adsorption on agricultural wastes-based activated carbons. *Fluid Phase Equilibria* **2012**, *317*, 9–14. [CrossRef]

53. Reffas, A.; Bernardet, V.; David, B.; Reinert, L.; Lehocine, M.B.; Dubois, M.; Batisse, N.; Duclaux, L. Carbons prepared from coffee grounds by H_3PO_4 activation: Characterization and adsorption of methylene blue and Nylosan Red N-2RBL. *J. Hazard. Mater.* **2010**, *175*, 779–788. [CrossRef] [PubMed]

54. Zhang, D.; Wang, T.; Zhi, J.; Zheng, Q.; Chen, Q.; Zhang, C.; Li, Y. Utilization of Jujube biomass to prepare biochar by pyrolysis and activation: Characterization, adsorption characteristics, and mechanisms for nitrogen. *Materials* **2020**, *13*, 5594. [CrossRef]

55. Rozada, F.; Otero, M.; Moran, A.; Garcia, A. Activated carbons from sewage sludge and discarded tyres: Production and optimization. *J. Hazard. Mater.* **2005**, *124*, 181–191. [CrossRef]

56. Daoud, M.; Benturki, O.; Girods, P.; Donnot, A.; Fontana, S. Adsorption ability of activated carbons from Phoenix dactylifera rachis and Ziziphus jujube stones for the removal of commercial dye and the treatment of dyestuff wastewater. *Microchem. J.* **2019**, *148*, 493–502. [CrossRef]

57. Msaada, A.; Belbahloula, M.; El Hajjajib, S.; Beakoua, B.H.; Houssainia, M.A.; Belhajjiaa, C.; Aassilac, H.; Zouhria, A.; Anouara, A. Industrial wastewater decolorization by activated carbon from Ziziphus lotus. *Desalin. Water Treat.* **2018**, *126*, 296–305. [CrossRef]

58. Angın, D. Effect of pyrolysis temperature and heating rate on biochar obtained from pyrolysis of safflower seed press cake. *Bioresour. Technol.* **2013**, *128*, 593–597. [CrossRef] [PubMed]

59. Adib, M.; Suraya, W.; Rafidah, H.; Amirza, A.; Attahirah, M.; Hani, M.; Adnan, M. Effect of phosphoric acid concentration on the characteristics of sugarcane bagasse activated carbon. *IOP Conf. Ser. Mater. Sci. Eng.* **2016**, *136*, 012061. [CrossRef]

60. Yakout, S.; El-Deen, G.S. Characterization of activated carbon prepared by phosphoric acid activation of olive stones. *Arab. J. Chem.* **2016**, *9*, S1155–S1162. [CrossRef]

61. Girgis, B.S.; El-Hendawy, A.-N.A. Porosity development in activated carbons obtained from date pits under chemical activation with phosphoric acid. *Microporous Mesoporous Mater.* **2002**, *52*, 105–117. [CrossRef]

62. Bahnes, Z.; Benderdouche, N.; Attouti, S.; Bestani, B.; Duclaux, L.; Reinert, L. Preparation of a novel activated carbon from jujube stones (*Ziziphus jujuba*) for the removal of basic and acid dyes. *Desalination Water Treat.* **2018**, *102*, 312–325. [CrossRef]

63. Chen, J.; Zhang, L.; Yang, G.; Wang, Q.; Li, R.; Lucia, L.A. Preparation and characterization of activated carbon from hydrochar by phosphoric acid activation and its adsorption performance in prehydrolysis liquor. *BioResources* **2017**, *12*, 5928–5941. [CrossRef]

64. Shahrokhi-Shahraki, R.; Benally, C.; El-Din, M.G.; Park, J. High efficiency removal of heavy metals using tire-derived activated carbon vs commercial activated carbon: Insights into the adsorption mechanisms. *Chemosphere* **2021**, *264*, 128455. [CrossRef] [PubMed]

65. Kundu, A.; Gupta, B.S.; Hashim, M.A.; Redzwan, G. Taguchi optimization approach for production of activated carbon from phosphoric acid impregnated palm kernel shell by microwave heating. *J. Clean. Prod.* **2015**, *105*, 420–427. [CrossRef]

66. El-Hendawy, A.-N.A. Variation in the FTIR spectra of a biomass under impregnation, carbonization and oxidation conditions. *J. Anal. Appl. Pyrolysis* **2006**, *75*, 159–166. [CrossRef]

67. Puziy, A.M.; Poddubnaya, O.I.; Martínez-Alonso, A.; Suárez-García, F.; Tascón, J.M.D. Synthetic carbons activated with phosphoric acid: I. Surface chemistry and ion binding properties. *Carbon* **2002**, *40*, 1493–1505. [CrossRef]

68. Hesas, R.H.; Arami-Niya, A.; Daud, W.M.A.W.; Sahu, J. Preparation and characterization of activated carbon from apple waste by microwave-assisted phosphoric acid activation: Application in methylene blue adsorption. *BioResources* **2013**, *8*, 2950–2966.

69. Solum, M.S.; Pugmire, R.J.; Jagtoyen, M.; Derbyshire, F. Evolution of carbon structure in chemically activated wood. *Carbon* **1995**, *33*, 1247–1254. [CrossRef]

70. Njewa, J.B.; Vunain, E.; Biswick, T. Synthesis and characterization of activated carbons prepared from agro-wastes by chemical activation. *J. Chem.* **2022**, *2022*, 9975444. [CrossRef]

71. Gunathilaka, H.; Thambiliyagodage, C.; Usgodaarchchi, L.; Angappan, S. Effect of surfactants on morphology and textural parameters of silica nanoparticles derived from paddy husk and their efficient removal of methylene blue. In Proceedings of the International Conference on Innovations in Energy Engineering & Cleaner Production (IEECP'21), San Francisco, CA, USA, 29–30 July 2021; pp. 29–30.

72. Sher, F.; Iqbal, S.Z.; Albazzaz, S.; Ali, U.; Mortari, D.A.; Rashid, T. Development of biomass derived highly porous fast adsorbents for post-combustion CO_2 capture. *Fuel* **2020**, *282*, 118506. [CrossRef]

73. Köseoğlu, E.; Akmil-Başar, C. Preparation, structural evaluation and adsorptive properties of activated carbon from agricultural waste biomass. *Adv. Powder Technol.* **2015**, *26*, 811–818. [CrossRef]

74. Djilani, C.; Zaghdoudi, R.; Modarressi, A.; Rogalski, M.; Djazi, F.; Lallam, A. Elimination of organic micropollutants by adsorption on activated carbon prepared from agricultural waste. *Chem. Eng. J.* **2012**, *189*, 203–212. [CrossRef]

75. Soedarmanto, H.; Sudjito, S.; Wijayanti, W.; Hamidi, N.; Setiawati, E. The impact of water soaking on physicochemical activated carbon produced by various thermal cracking temperature. *AIP Conf. Proc.* **2020**, *2278*, 020008.

76. Girgis, B.S.; Temerk, Y.M.; Gadelrab, M.M.; Abdullah, I.D. X-ray diffraction patterns of activated carbons prepared under various conditions. *Carbon Sci.* **2007**, *8*, 95–100. [CrossRef]

77. Açıkyıldız, M.; Gürses, A.; Karaca, S. Preparation and characterization of activated carbon from plant wastes with chemical activation. *Microporous Mesoporous Mater.* **2014**, *198*, 45–49. [CrossRef]

78. Rahman, A.; Hango, H.J.; Daniel, L.S.; Uahengo, V.; Jaime, S.J.; Bhaskaruni, S.V.; Jonnalagadda, S.B. Chemical preparation of activated carbon from Acacia erioloba seed pods using H_2SO_4 as impregnating agent for water treatment: An environmentally benevolent approach. *J. Clean. Prod.* **2019**, *237*, 117689. [CrossRef]

79. Aragaw, T.A.; Asmare, A.M. Phycoremediation of textile wastewater using indigenous microalgae. *Water Pract. Technol.* **2018**, *13*, 274–284. [CrossRef]

80. Hossain, M.S.; Sarker, P.; Rahaman, M.S.; Uddin, M.K. Integrated performance of Fenton process and filtration (Activated Charcoal and Sand) for textile wastewater treatment. *Curr. J. Appl. Sci. Technol.* **2020**, *39*, 21–31. [CrossRef]

81. Farch, S.; Yahoum, M.M.; Toumi, S.; Tahraoui, H.; Lefnaoui, S.; Kebir, M.; Zamouche, M.; Amrane, A.; Zhang, J.; Hadadi, A. Application of Walnut Shell Biowaste as an Inexpensive Adsorbent for Methylene Blue Dye: Isotherms, Kinetics, Thermodynamics, and Modeling. *Separations* **2023**, *10*, 60. [CrossRef]

82. Jawad, A.H.; Saber, S.E.M.; Abdulhameed, A.S.; Farhan, A.M.; ALOthman, Z.A.; Wilson, L.D. Characterization and applicability of the natural Iraqi bentonite clay for toxic cationic dye removal: Adsorption kinetic and isotherm study. *J. King Saud Univ. -Sci.* **2023**, *35*, 102630. [CrossRef]

83. Karim, M.E.; Dhar, K.; Hossain, M.T. Physico-Chemical and Microbiological Analysis of Textile Dyeing Effluents. *IOSR J. Environ. Sci. Toxicol. Food Technol. (IOSR-JESTFT)* **2015**, *9*, 2319–2399.

84. Prado, E.; Miranda, F.; de Araujo, L.; Fernandes, G.; Pereira, A.J.; Gomes, M.; da Silva Sobrinho, A.; Baldan, M.; Petraconi, G. Physicochemical Modifications and Decolorization of Textile Wastewater by Ozonation: Performance Evaluation of a Batch System. *Ozone Sci. Eng.* **2022**, *45*, 276–290. [CrossRef]

85. Pavithra, M.; Kousar, H. Characterization of certain physico-chemical parameters of textile waste water. *Int. J. Environ. Sci.* **2016**, *5*, 39–41.

86. Tafesse, T.; Yetemegne, A.; Kumar, S. BThe Physico-Chemical Studies of Wastewater in Hawassa Textile Industry. *J. Environ. Anal. Chem.* **2015**, *2*, 4. [CrossRef]

87. Baral, A.; Das, D.P.; Minakshi, M.; Ghosh, M.K.; Padhi, D.K. Probing Environmental Remediation of RhB Organic Dye Using α-MnO_2 under Visible-Light Irradiation: Structural, Photocatalytic and Mineralization Studies. *ChemistrySelect* **2016**, *1*, 4277–4285. [CrossRef]

88. Ahmad, A.; Hameed, B. Reduction of COD and color of dyeing effluent from a cotton textile mill by adsorption onto bamboo-based activated carbon. *J. Hazard. Mater.* **2009**, *172*, 1538–1543. [CrossRef]

89. Tebeje, A.; Worku, Z.; Nkambule, T.; Fito, J. Adsorption of chemical oxygen demand from textile industrial wastewater through locally prepared bentonite adsorbent. *Int. J. Environ. Sci. Technol.* **2021**, *19*, 1893–1906. [CrossRef]

90. Zaharia, C.; Suteu, D. Coal fly ash as adsorptive material for treatment of a real textile effluent: Operating parameters and treatment efficiency. *Environ. Sci. Pollut. Res.* **2013**, *20*, 2226–2235. [CrossRef]

91. Khellouf, M.; Chemini, R.; Salem, Z.; Khodja, M.; Zeriri, D.; Jada, A. A new activated carbon prepared from cypress cones and its application in the COD reduction and colour removal from industrial textile effluent. *Environ. Dev. Sustain.* **2021**, *23*, 7756–7771. [CrossRef]

92. Elayadi, F.; Achak, M.; Boumya, W.; Elamraoui, S.; Barka, N.; Lamy, E.; Beniich, N.; El Adlouni, C. Factorial Design Statistical Analysis and Optimization of the Adsorptive Removal of COD from Olive Mill Wastewater Using Sugarcane Bagasse as a Low-Cost Adsorbent. *Water* **2023**, *15*, 1630. [CrossRef]

93. Santhy, K.; Selvapathy, P. Removal of reactive dyes from wastewater by adsorption on coir pith activated carbon. *Bioresour. Technol.* **2006**, *97*, 1329–1336. [CrossRef]